Synthetic diagnostics for interpretation of ICF experiments using hydrodynamic simulations

L. Antonelli, S. Atzeni, A. Schiavi

Dipartimento SBAI, Università di Roma "La Sapienza", Roma, Italy

1. Introduction

The design and interpretation of inertial confinement fusion and high energy density experiments rely heavily on multi-dimensional radiation-hydrodynamic simulations. Code main output typically consists of sequences of maps of fluid and thermodynamic variables, which are not easily compared with experimental observables. More direct comparison requires the development of simulated, or synthetic, diagnostics, using the detailed plasma information available in the fluid simulations. This has motivated the development of a set of simulated diagnostics coupled, either on-line or off-line, to our 2D Lagrangian code DUED [1, 2].

We report on two new software tools: x-ray radiography [3] for shock compression of matter and fast charged particle spectrometry for stopping power measurements. In addition, we are developing synthetic streaked optical pyrometry and we are improving neutron spectrometry software, already partly described in Ref. [4], and recently used to interpret exploding pusher experiments [5].

2. X-radiography

Pulsed x-ray absorption radiography (e.g. [6, 7]) is a powerful technique to diagnose matter compressed by strong laser-driven shock waves, and in particular to obtain such information as shock wave position and shape, and shock compression ratio. Analysis of x-radiography is usually based on Abel inversion, which however cannot take into account the finite size of the x-ray source and the specific experimental geometry. In order to overcome some of these limitations we have developed a synthetic diagnostic tool, coupled to DUED. The importance of accounting for the finite size of the x-ray source is clearly shown by Fig. 1, referring to a radiograph of a cold, uncompressed hemisphere of plastic. It is seen that the experimental transmission profile is only reproduced when considering x-ray source FWHM of about 30 μm. Details about application of the technique to shock wave characterization are given in a separate publication [3], where it is shown that comparison between experimental and synthetic radiographs allows to infer properties of the shocked material. Just as an example, in Fig. 2 we compare an experimental radiograph of and a simulated one. They refer to a curved shock wave in a cylindrical target [3].
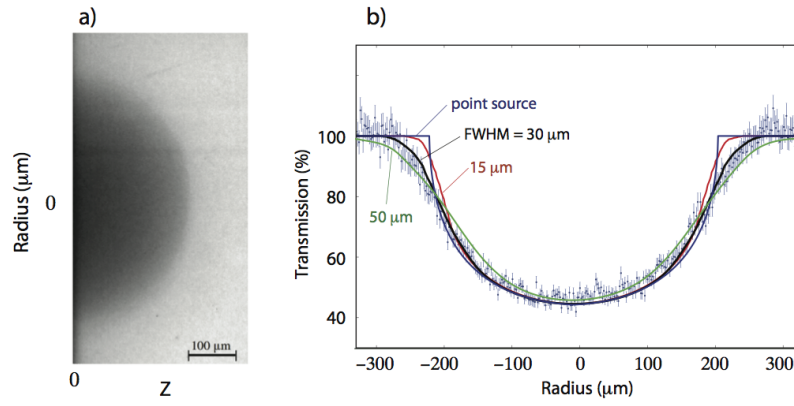
Figure 1: *Radiograph of a hemisphere. a) experimental radiograph from Ref. [3]; b) Transmission maps along the line $z = 130\,\mu m$. Points: experimental data; curves: simulated transmission, for different values of the source FWHM. (Once reduced the experimental noise, Abel inversion would produce the same curve as that for the point source.)*
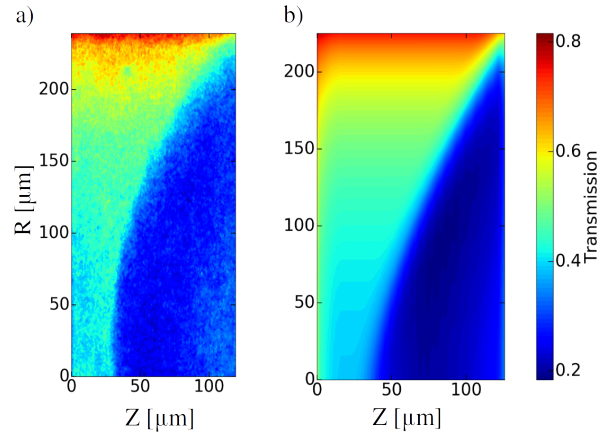

Figure 2: *Experimental radiograph (a) and simulated radiograph (b). Matter is compressed by a shock-wave progressing from right to left.*

3. Fast proton spectra

Proton stopping power (and more generally, ion stopping power) strongly depends on particle energy, target density and, in a plasma, target temperature. See Fig. 3, referring to protons in Argon, computed using a model similar to that of Ref. [8], modified to reproduce SRIM's [9] cold matter limit. So far, very limited experimental data have been obtained on stopping power in a plasma, due to the difficulty of generating a sufficiently large (in terms of ρL), uniform and well characterized hot plasma. In principle, measurements can be performed by using a gas jet as a target. A nearly monochromatic proton beam is sent through the jet along an axis orthogonal to the jet. In addition, the jet can be heated by a laser pulse orthogonal to both jet and proton beam [10, 11]. A similar configuration is used in the tool coupled to DUED. However, while the
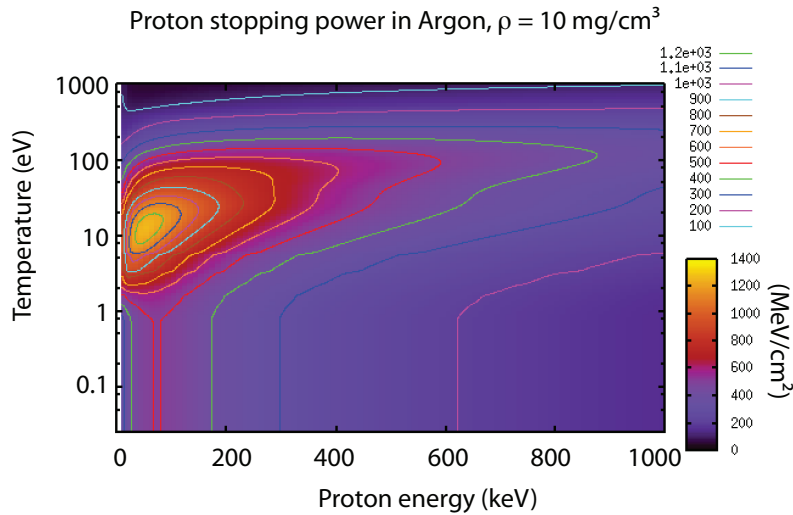
Proton stopping power in Argon, $\rho = 10$ mg/cm^3

Figure 3: *Map of proton stopping power in Argon at density of 10 mg/cm^3.*

experimental set-up is 3D, simulations are 2D, and are performed in the plane transverse to jet axis, either in Cartesian (slab) coordinates or cylindrical coordinates (with rotational symmetry around the laser axis).

The results of a few illustrative simulations are presented in Fig. 4, showing both target density and temperature maps, as well as input and output proton spectra. The results for the cold gas are in agreement with simple models [11] and with SRIM's data. In the case of a target at 600 eV uniform temperature, the spectrum peaks at higher energy than in the cold-gas case, because a hot plasma is a less effective stopper than cold matter. The laser-heated case is more complex, due to non-uniform heating and shocks; in addition in this case the spectrum changes rapidly in time during laser irradiation. Detailed comparison with experiments will be published elsewhere [9].

References

[1] S. Atzeni, Comput. Phys. Commun **43**, 107 (1986)

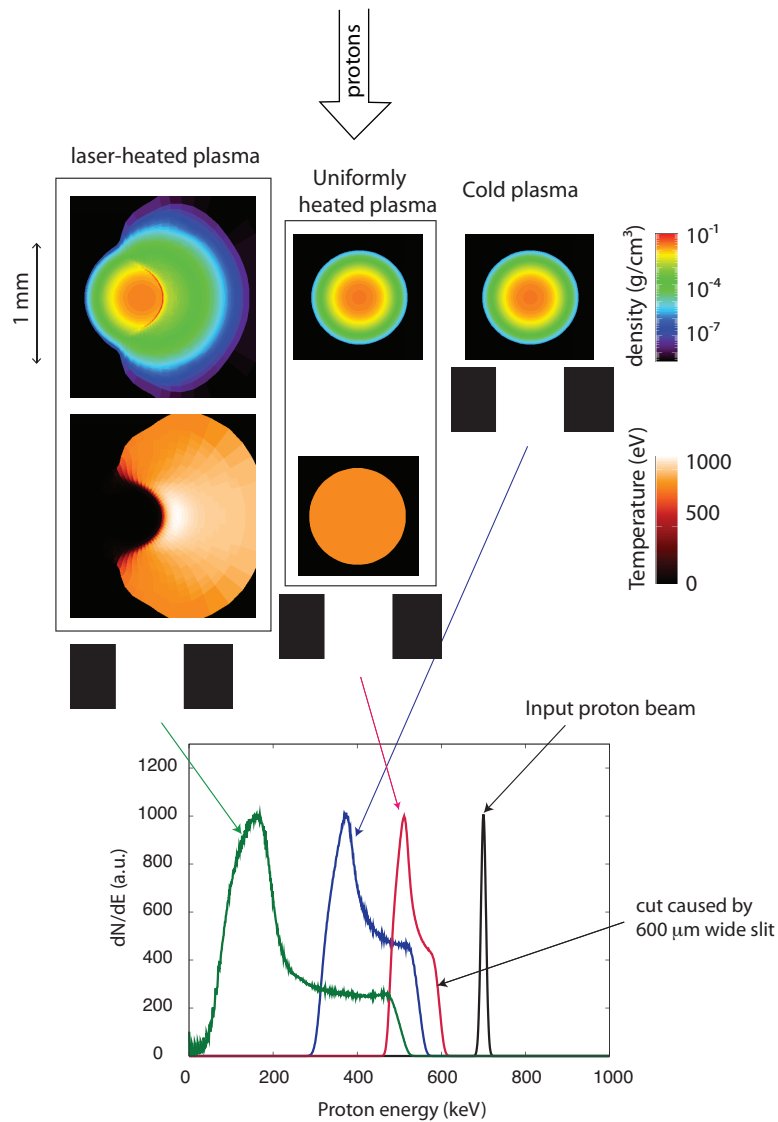[2] S. Atzeni *et al.*, Comput. Phys. Commun **106**, 153 (2005)

Figure 4: *Simulated protons spectra.*

[3] L. Antonelli *et al.*, Phys. Rev. E **95**, 063205 (2017)

[4] S. Atzeni and G. Rossi, Proc. 42nd EPS Conf. on Plasma Physics (2015), P1.203

[5] O. Larroche *et al.*, Phys. Plasmas **23**, 012701 (2016)

[6] A. Benuzzi *et al.*, Phys. Rev. E **77**, 045402 (2008)

[7] S. Hu *et al.*, Phys. Rev. Lett. **100**, 185003 (2008)

[8] M. Basko, Sov. J. Plasma Phys. **10**, 109 (1984)

[9] J. F. Ziegler et al., *Stopping power and range of Ions in Matter*, www.srim.org

[10] S. N. Chen *et al.* NIMA **740**, 105 (2014)

[11] S. N. Chen *et al.* Experimental measurements of proton stopping power on passing through
       a hot plasma, in preparation